

Semi-automatic classification of tree species in different forest ecosystems by spectral and geometric variables derived from Airborne Digital Sensor (ADS40) and RC30 data

L. T. Waser^{1*}, C. Ginzler¹, M. Kuechler¹, E. Baltsavias², L. Hurni³

¹ Swiss Federal Research Institute WSL, Land Resources Assessment, 8903 Birmensdorf, Switzerland

² Institute of Geodesy and Photogrammetry, ETH Zurich, 8093 Zurich, Switzerland

³ Institute of Cartography, ETH Zurich, 8093 Zurich, Switzerland

*Corresponding author; e-mail: lars.waser@wsl.ch

Abstract

This study presents an approach for semi-automated classification of tree species in different types of forests using first and second generation ADS40 and RC30 images from two study areas located in the Swiss Alps. In a first step, high-resolution canopy height models (CHMs) were generated from the ADS40 stereo-images. In a second step, multi-resolution image segmentation was applied. Based on image segments seven different tree species for study area 1 and four for study area 2 were classified by multinomial regression models using the geometric and spectral variables derived from the ADS40 and RC30 images. To deal with the large number of explanatory variables and to find redundant variables, model diagnostics and step-wise variable selection were evaluated. Classifications were ten-fold cross-validated for 517 trees that had been visited in field surveys and detected in the ADS40 images. The overall accuracies vary between 0.76 and 0.83 and Cohen's kappa values between 0.70 and 0.73. Lower accuracies ($\text{kappa} < 0.5$) were obtained for small samples of species such as non-dominant tree species or less vital trees with similar spectral properties. The usage of NIR bands as explanatory variables from RC30 or from the second generation of ADS40 was found to substantially improve the

classification results of the dominant tree species. The present study shows the potential and limits of classifying the most frequent tree species in different types of forests, and discusses possible applications in the Swiss national forest inventory.

30

Keywords: airborne digital sensor, canopy height model, forest inventory, multinomial regression, multi-sensor integration, tree species

33

Abbreviations: ADS (Airborne Digital Sensor), BRDF (bidirectional reflectance distribution function), CHM (canopy height model), CIR (color-infrared), DSM (digital surface model), DTM (digital terrain model), GLM (generalized linear model), IHS (intensity, hue, saturation), NFI (national forest inventory), NIR (near-infrared), RC30 (aerial row camera), VHR (very high resolution)

38

1. Introduction

40

Precise information on species composition is essential for forest studies, inventories, management and other forest applications. Tree species maps of forest ecosystems are a required input for biodiversity and biomass estimations and therefore indispensable for many environmental, monitoring or protection tasks.

Historically, aerial photography represents the most popular input to remote sensing in forestry (Spurr, 1960; Gillis and Leckie, 1996). Classification of tree species was based on the interpretation and mapping of aerial photographs (i.e. acquired from RC30) and methods have been developed to identify the individual tree crowns (Wulder, 1998; Bolduc et al., 1999; Erikson, 2004). In recent years, high spatial resolution images have been used to obtain information on individual tree species (Brandtberg, 2002; Key et al., 2001; St-Onge et al., 2004). With the increasing availability of digital airborne imagery, a new round of research on classifying tree species on individual tree level is being initiated. Digital airborne data have facilitated new opportunities for tree species classification since the digital devices are supposed to be spectrally and radiometrically superior to the analogue cameras (Petrie and Walker, 2007). The data are recorded by frame-based sensors, e.g. Z/I DMC (Olofsson et

53 al., 2006; Holmgren et al., 2008), Ultracam (Hirschmugl et al., 2007) or line-scanning sensors, e.g. ADS40 /
54 ADS80 (Waser et al., 2010), which provide stereo-overlap of up to 90% or entire image strips with higher
55 radiometric resolution.

56 Great progress is occurring in three-dimensional remote sensing including digital stereo-photogrammetry, radar
57 interferometry and LiDAR. By subtracting, for example, a digital terrain model (DTM) from the corresponding
58 digital surface model (DSM), canopy height models (CHMs) can be calculated that provide a basis for
59 estimating forest attributes like height, area or tree species composition. In recent years, especially high
60 resolution airborne laser scanning (ALS) has become an operational tool for producing forest inventory data in
61 many countries and also species classification has become feasible (Brandtberg, 2007; Holmgren and Persson,
62 2004; Ørka et al., 2009).

63 Several studies reveal that combining optical data with 3-D information obtained from CHMs for the extraction
64 of trees (Straub, 2003; St-Onge et al., 2004; Hirschmugl et al., 2007; Waser et al., 2008a & 2008b) or tree
65 species classification lead to better accuracies than using only a single data input (Heinzel et al., 2008;
66 Holmgren et al., 2008; Lamonaca et al., 2008; Chubey et al., 2009).

67 According to Jensen (2005) the most appropriate classification strategy depends on different parameters such as
68 the biophysical characteristics of the research area, the homogeneity of the remote sensing data and the “a
69 priori” knowledge. Several studies stress the advantages of combining multi-resolution segmentation (Batz and
70 Schäpe, 2000) with object-based classification (De Kok and Wezyk, 2006; Wang et al., 2006; Lamonaca et al.,
71 2008) to fully explore the information content of VHR images.

72 According to Guisan and Zimmermann (2000) or Scott et al. (2002), modern regression approaches such as
73 generalized linear models (GLMs) have proven particularly useful for modeling the spatial distribution of plant
74 species and communities (Guisan et al., 2004). The growing need for sensitive tools to predict spatial and
75 temporal patterns of plant species or communities (Guisan and Thuiller, 2005) is reflected by an increasing
76 usage of predictive spatial modeling over the past 20 years. Küchler et al. (2004) show that spatially explicit
77 predictive modeling of vegetation using remotely sensed environmental attributes can be used to construct
78 current vegetation cover. Thus multinomial regression models seem especially promising for modeling tree

species when analyzing the relationship between categorical dependent variables (e.g. tree species) and explanatory variables derived from remotely sensed data (Waser et al., 2008b & 2008c).

The objective of this study was to develop a robust semi-automated classification method for the most frequent tree species (at least 5% coverage according to the Swiss NFI) in two study areas with different types of forests, and to show the potential of first and second generation ADS40 imagery. A drawback for study area 1 is that the NIR channel of the 1st generation ADS40 data from 2005 was not available. CIR RC30 images were used instead. The study was carried out within the framework of the Swiss National Forest Inventory (NFI) (Brassel and Lischke, 2001) and the Swiss Mire Protection Program (Ecker et al., 2008).

In the current study, a multinomial model has been developed for two study areas of few square kilometers but that are representative for heterogeneous forest regions concerning both topography and tree species composition. Since for the Swiss NFI and for monitoring biotopes of national importance, tree species composition of greater areas, preferably on the national scale are required, this preliminary study is a first important contribution. The continuity of this approach will be guaranteed since the required input data (field samples, images) is being provided by other national campaigns or monitoring programs. The image data from a second generation ADS40 and an ADS80 sensor (follow-up product of ADS40 since 2009) will be available every three years nationwide.

2. Material

2.1 Study areas

Study area 1 is located in the pre-alpine zone (approx. 47°18' N and 9°14' E) and is approx. 2.4 km² in area. The terrain varies (steep slopes and flat areas) with mixed land cover such as forest and wetlands. The altitude ranges from 900 m to 1350 m a.s.l. The forest area covers approx. 1.5 km², and is mostly characterized by mixed forest with a dominance of deciduous trees along the creeks. The dominating deciduous tree species are *Fagus sylvatica* and *Fraxinus excelsior* and less frequently *Acer sp.*, *Alnus sp.*, and *Betula sp.* The main coniferous trees are *Abies alba* and *Picea abies*.

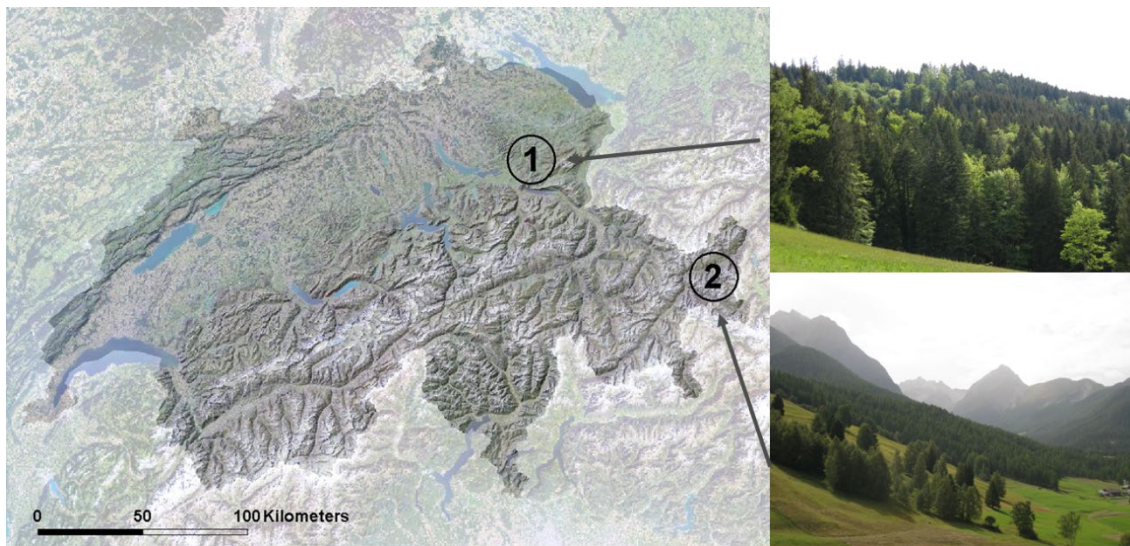


Figure 1. Left: Shaded relief and Landsat TM images of Switzerland (© 2006 Swisstopo JD052552). Top right: study area 1 (Pre-Alps); bottom right: study area 2 (Central Alps).

Study area 2 is located in the Central Alps (approx. 46°46' and 10°16'), and is approx. 4.2 km² in area. It includes steep terrain which is mostly north oriented (Fig. 1). The altitude ranges from 1250 m to 2050 m a.s.l. It is characterized by large forests, with some pastures and wetlands in the centre. The forest covers 2.8 km² and is mostly mixed forest in the lower parts and coniferous mountain forest with very old stands in the upper parts. The dominating tree species are *Larix decidua*, *Picea abies*, *Pinus sylvestris* and *Betula sp.*

2.2 Ground truth

The ground truth data to validate the tree species classifications was collected in the natural environment to be representative for both study areas. A variety of tree species communities are present in each study area. Two ground surveys were carried out in summer 2008 in each study area, focusing on the most frequent tree species (at least 5% coverage in Switzerland) which were also visible in the aerial images. For a total of 285 sampled

124 trees in study area 1 and 232 in study area 2 we recorded the species (table 1) and determined the tree position
 125 with a sub-decimeter GPS with differential correction (Leica TPS1200). Additionally, the crowns of all visited
 126 trees were delineated in the field on the corresponding aerial images. This information together with the
 127 measured XY positions was used as reference to digitize the corresponding tree crowns on the ADS40 RGB
 128 images. Typical examples of each tree species as seen in the ADS40 RGB images are shown in Fig. 2. This
 129 information was used to calibrate and validate the multinomial regression models. Species information from
 130 Swiss NFI terrestrial surveys on sample plot level was not used in this study because the exact position of the
 131 sample centers was unknown. Since last summer, the center point of each visited sample plot is measured with a
 132 GPS (Trimble Geoexplorer XH). The exact positions relative to the plot center of all trees are known: they have
 133 been measured using measuring bands and compass.

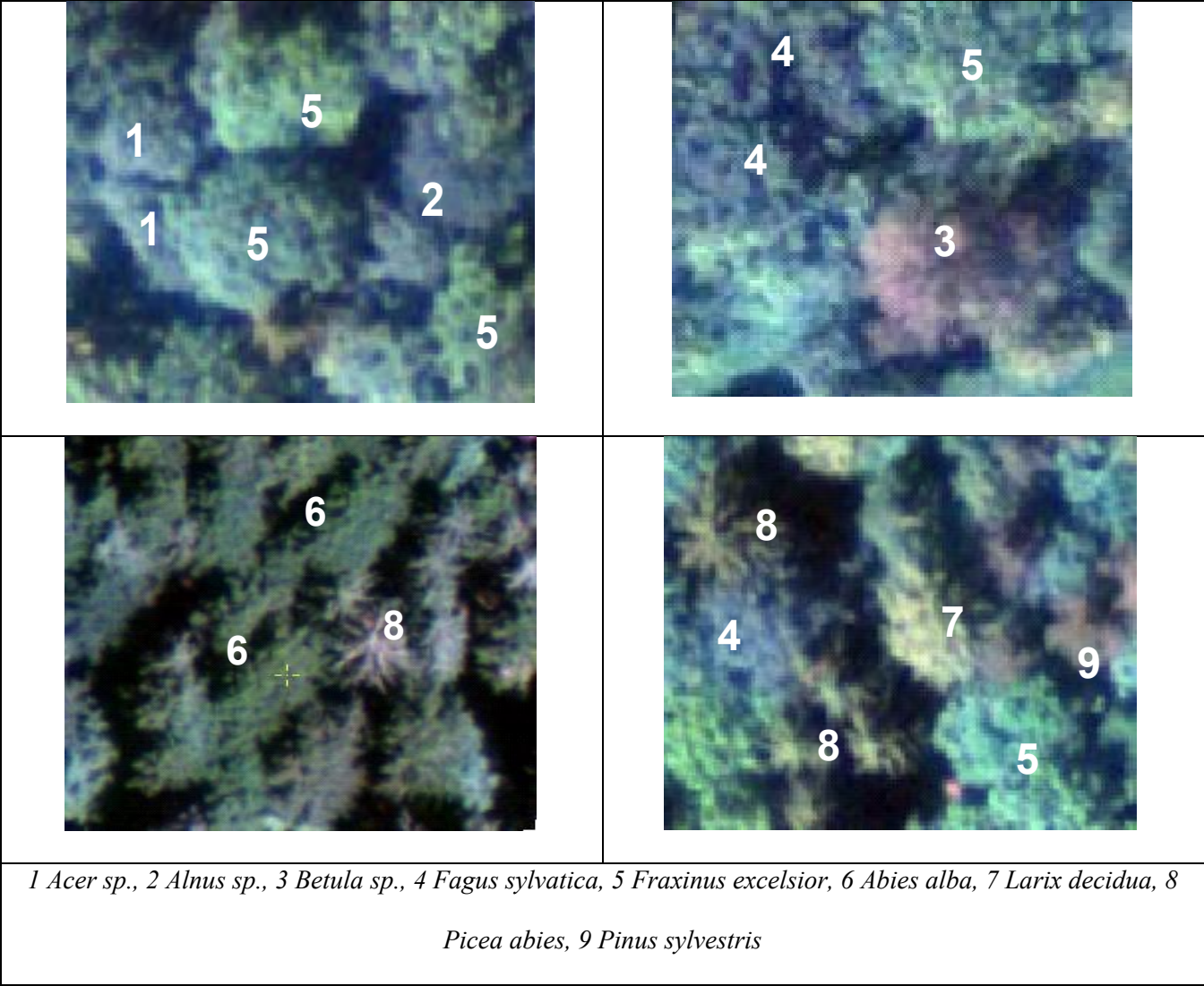
134

135 **Table 1.** Tree species sampled in the two study areas. Species proportion of tree species is based on estimates by an expert during the
 136 field surveys, (similar tree species of study area 2 in brackets).

Scientific tree species name	Common tree species name	Number of samples	Species proportion	Study area
<i>Acer sp.</i>	maple	20	< 10%	1
<i>Alnus sp.</i>	alder	21	10%	1
<i>Betula sp.</i>	birch	21 (39)	<10%	1, 2
<i>Fagus sylvatica</i>	beech	52	20%	1
<i>Fraxinus excelsior</i>	ash	56	15%	1
<i>Abies alba</i>	white fir	51	15%	1
<i>Larix decidua</i>	larch	87	50%	2
<i>Picea abies</i>	Norway spruce	64 (44)	25% (10%)	1, 2
<i>Pinus sylvestris</i>	Scots pine	62	30%	2

137

138



139

140 **Figure 2.** Examples of the 9 collected tree species as they appear in the ADS40 RGB imagery.

141

142 2.3 Remotely sensed data

143 This study uses three different sets of input data types: 1. ADS40 (first and second generation) images, 2. RC30
 144 CIR aerial images and 3. LiDAR DTMs. All datasets were resampled to 0.25 m for study area 1 and 0.5 m for
 145 study area 2. Table 2 lists the image data and their characteristics as used in this study. The RC30 images are
 146 only available for selected areas on request, unlike the ADS40 images, which are available for the whole of
 147 Switzerland.

148

149 2.3.1 *Airborne Digital Sensor data (ADS40)*

150 First generation ADS40-SH40 and second generation ADS40-SH52 images Level 1 (Leica Geosystems AG,
151 Switzerland) were used in this study (for further details on the sensor see e.g. Reulke et al. 2006). For technical
152 details and descriptions of earlier applications, see Kellenberger et al. (2007) and Kellenberger and Nagy (2008).
153 The main drawback of the first-generation ADS40-SH40 is that the NIR line CCD is placed 18° forward from
154 the nadir RGB CCDs which makes it difficult to combine all four lines. The second generation ADS40-SH52
155 provides the NIR band in the same nadir position as the RGB bands. ADS40-SH52 data had been collected only
156 for study area 2 when this study was carried out. For both study areas, digital surface models (DSMs) were
157 generated automatically from the above images with a spatial resolution of 0.5 m using modified strategies of
158 NGATE of SOCET SET 5.4.1 (BAE Systems). Prior to the DSM generation, a Wallis filter is applied to
159 enhance contrast, especially in shadow regions, and to equalize radiometrically the images for matching.
160 NGATE performs image correlation and edge matching on each image pixel. Based on a hybrid approach, it
161 uses both area-matching and edge-matching. Baltsavias et al. (2008) encountered some problems applying these
162 matching strategies especially for forests and open vegetation lands since they were primary developed for
163 urban areas. They suggest using a new, high-quality multi-image matching method (implemented in the program
164 package SAT-PP), but this matching method is still under development for ADS40 image data (Zhang and
165 Gruen, 2004).

166

167 2.3.2 *Scanned CIR aerial images*

168 For study area 1, five consecutive colour infrared (CIR) aerial film images were acquired with an Leica RC30
169 camera. They were digitized with a Vexcel UltraScan and 15 µm pixel size. Image orientation was established
170 with 20 ground control points, previously measured in a differential GPS survey, using bundle adjustment
171 (Socet Set 5.4.1 of BAE Systems).

172

173 **Table 2.** Summary of characteristics of the image data used

174

Sensor	CIR RC30	ADS40-SH40	ADS40-SH52
Study area	1	1	2
Acquisition date	2005/08/08	2005/08/12	2008/09/02
Mapping Scale	1:5,700	~1:15,000	~1:20,000
Focal length	300 mm	62.8 mm	62.8 mm
Spectral resolution (nm)	Green: 500-600 Red: 600-700 NIR: 750-1000	Red: 610-660 Green: 535-585 Blue: 430-490	Red: 608-662 Green: 533-587 Blue: 428-492 NIR: 833-887
Ground pixel size	~8.5 cm	~25 cm	~50 cm
Orthoimage	25 cm	25 cm	50 cm
Radiometric resolution	8 bit --	11 bit 12,000 pixels / array	11 bit 12,000 pixels / array

175

176

177 2.3.3 LiDAR data

178 National LiDAR digital terrain data (DTM) produced by the Swiss Federal Office of Topography
179 (SWISSTOPO) for study area 1 (acquisition date: March 2002, reflight October 2002, leaves-off) and study
180 area 2 (March 2003, reflight October 2003, partly leaves-off) were used. The data were acquired by Swissphoto
181 AG / TerraPoint using a TerraPoint ALTMS 2536 system with an average flying height above ground of 1200
182 m. The DTM has an average point density of 0.8 points / m² and height accuracy (1 sigma) of 0.5 m (Artuso et
183 al. 2003) and was interpolated to a regular grid with 0.25 m (study area 1) and 0.5 m (study area 2) grid spacing.

184

185 3. Methods

186

187 The models have been developed and tested in the two forest ecosystems in Switzerland as shown in Fig. 1. The
188 main steps in processing the data and the methodological workflow are given in Fig. 3.

189

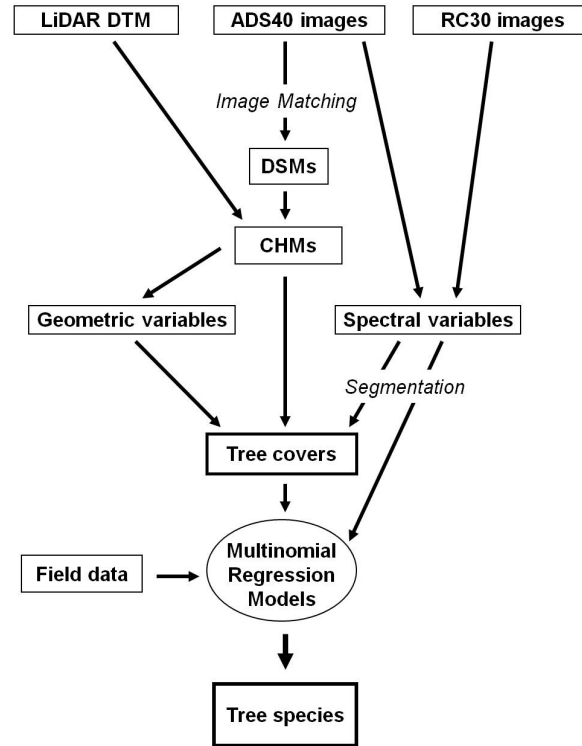


Figure 3. Overview of the methodological workflow, with the main processing steps.

3.1 Variables derived from remotely sensed information

To extract tree area and classify tree species, several variables (geometric and spectral signatures) were derived from the remote sensing data using standard digital image processing methods as described in Gonzales and Woods (2002). Details about extraction of geometric and spectral explanatory variables derived from airborne remote sensing data are described in Waser et al. (2007 & 2008a). Geometric variables are often used in hydrological or geomorphologic analyses of land surface and topography. They can also be used to describe the physical characteristics of natural and artificial objects of a digital surface model. They can support image segmentation or improve the distinction between, e.g. trees and roofs, in a forest classification process. The input variables used in this study consist of four commonly used geometric parameters derived from the CHMs (slope, curvature, and two local neighborhood functions). For further details, see table 3, Burrough (1986) and Moore et al. (1991). As spectral variables (see table 3) we produced the mean and standard deviations of: 3 x 3 original bands of ADS40-SH40, ADS40-SH52 and RC30 CIR; the 3 ratios of each band, i.e. red band divided

205 by the sum of the corresponding three bands; and the color transformation from RGB and CIR to IHS (for RC30
 206 only CIR to IHS) into the 3 channels intensity (I), hue (H), and saturation (S). The NIR information from the
 207 RC30 CIR images was used as the explanatory variable to test for possible benefits of the NIR information
 208 provided by second generation ADS40 imagery.

209

210 **Table 3.** Overview of the explanatory variables produced to classify the tree species in the two study areas

211

Source	Variable	Description	Study area
Canopy height model	slope	Rate of maximum change in z value from each cell	1, 2
	curvature	Curvature of a surface at each cell centre (3x3 window)	1, 2
	plan	Rate of change in slope for each cell. Curvature of the surface in the direction of slope (3x3 window)	1, 2
	prof	Assessment of topographic position (four classes: ridge, slope, toe slope and bottom). The resulting grid displays the most extreme deviations from a homogeneous surface.	1, 2
ADS40-SH40 / SH52 images	original bands RGB	1. band: red, 2. band: green, 3. band: blue	1, 2
	ratios of RGB bands	Red / (red + green + blue); green / (red + green + blue); blue / (red + green + blue)	1, 2
	IHS of RGB	transforms red, green, and blue values into intensity, hue, and saturation	1, 2
ADS40-SH52	original bands CIR	1. band: NIR, 2. band: red, 3. band: green	2
	ratios of CIR bands	NIR / (NIR + red + green); red / (NIR + red + green); green / (NIR + red + green)	2
	IHS of CIR	transforms red, green, and NIR values into intensity, hue, and saturation	2
RC30 images	original bands CIR	“	1
	ratios of CIR bands	“	1
	IHS of CIR	“	1
Σ	22		1, 2

212

213

214 *3.2 Image segmentation*

215 Homogenous image segments of individual tree crowns or tree clusters are needed to classify tree species (see
216 below). Both the ADS40-SH40 and /ADS40-SH52 orthoimages were therefore subdivided into patches by a
217 multi-resolution segmentation using the Definiens 7.0 software (Batz & Schäpe, 2000). The RGB bands were
218 used as input data with the DSMs providing additional geometric information (height and slope). Segmentation
219 was iteratively optimized using several levels of detail and adapted to shape and compactness parameters. The
220 final segmentation provides groups of trees and individual trees with similar shapes and spectral properties.
221 Finally, the means and standard deviations of the geometric and spectral variables were calculated for each
222 segment.

223

224 *3.3. Tree covers*

225 The extraction of the area covered by trees is required for the area-wide mapping of the tree species. Tree cover
226 and non-tree area masks were generated in four steps. First, for each study area a digital canopy height model
227 (CHM) was produced subtracting the LiDAR DTM from the DSMs. In a second step, pixels with CHM values \geq
228 3 m were used to extract potential tree areas according to the definition in the Swiss NFI (Brassel and Lischke,
229 2001). In a third step, non-tree objects, e.g. buildings, rocks, and artifacts were removed using spectral
230 information from the ADS40-SH52 CIR and RC30 CIR images (low NDVI pixel values) as well as information
231 (curvature) about the image segments (e.g. segments on buildings have lower curvature values and ranges than
232 trees or large shrubs). These four steps resulted in two canopy covers providing sunlit tree area for each study
233 area.

234

235 *3.4 Classification of tree species*

236 *3.4.1 Modeling procedures*

237 Image segments representing single trees were to be assigned to classes (species) by predictive modeling. The
238 classes were given by a field sample from the 7 respectively 4 dominant tree species of the study areas as

described in section 2.2. As each response variable has more than two possible states, a multinomial model had to be applied. Multinomial logistic regression as described in detail in Hosmer and Lemeshow (2000) was used to assign the segments to the species with the highest modeled probability.

In multinomial logistic regression, one category of the dependent variable is chosen as the comparison category. Separate relative risk ratios are determined for each category of the response variable with the exception of the comparison category, which is omitted from the analysis. The formula of the multinomial logistic regression function is given in equations 1 and 2:

$$P(y_i = r) = \frac{\exp(X_i \beta_r)}{1 + \sum_{r=1}^J \exp(X_i \beta_r)} \quad (1)$$

and

$$P(y_i = 0) = \frac{1}{1 + \sum_{r=1}^J \exp(X_i \beta_r)} \quad (2)$$

where for the i th individual Y_i is the response variable (one of the tree species), X_i is a vector of the explanatory variables (geometric data, image bands and derivatives given in section 3.1), β_j is the unknown corresponding parameter (estimated by maximum likelihood). J is the number of categories (4 or 7 tree species) and r is the tree species tested.

In R version 2.11.0, several algorithms for multinomial models are available. The R package *nnet* provides an implementation on the base of a neuronal network which is very robust with respect to redundant explanatory variables, but which does not output detailed model diagnostics (only AIC and deviance of the whole model). The algorithm *mlogit* provides extensive model diagnostics, but fails if variables are collinear or differently redundant.

3.4.2 Variable selection and validation

258 A good fit to the given (training) data is not a sufficient condition for good predictive models. Particularly when
259 many explanatory variables are used with relatively few observations, the result is an excellent fit to the training
260 data, but poor predictions for additional data. To obtain good predictions, a small set of powerful variables has
261 to be selected. Step-wise selection procedures have been developed and optimized for linear models. These
262 procedures can also be applied to other model types, but the results have to be considered with reservation
263 (Guisan et al. 2002). Therefore some additional effort was taken to assess the explanatory power of the
264 variables.

265 The mean and standard deviations of the explanatory variables were grouped as follows: First, the variables IHS
266 of the RGB and CIR bands because they are supposed to concentrate a maximum of information in few
267 channels, second the variables obtained from the original color bands and the ratios of the original bands to
268 provide information lost by the IHS transformation, third the geometric variables to provide information which
269 is not given by the spectral variables. The explanatory variables were tested in three ways: 1) The significant
270 terms within each variable group for each tree species as provided by the *mlogit* output were counted.
271 Redundant variables (one of the three ratio channels and some of the geometric variables, see tables 5 and 6) had
272 to be omitted to prevent failure of *mlogit*. 2) Step-wise variable selection was applied (AIC, both directions,
273 Akaike, 1973) on separate logistic models for each tree species. Then, the terms remaining in the models were
274 counted for each variable group and tree species. 3) Finally, the predictive power of the models was verified by
275 a ten-fold cross-validation. The statistical measures used to validate the results were: producer's- and user's
276 accuracy, correct classification rate (*CCR*), kappa coefficient (*K*). In summary, the assignment of tasks and R-
277 functions was the following:

- 278 • Testing the explanatory power of the variables: *mlogit*
- 279 • Step-wise variable selection: separate logistic models
- 280 • Cross-validation: *nnet*

281

282 3.4.3 Assignments of field samples to aerial images

283 In order to validate the predictions of tree species, the digitized reference tree data (see section 2.2) had to be
 284 assigned to the corresponding image segments. However, the delineations of the field samples were not always
 285 (or even rarely) congruent with the automatically generated image segments. Each of the digitized reference
 286 trees (285 in study area 1 and 232 in study area 2) was assigned to an image segment using the following rule: If
 287 one segment contained more than one digitized field sample, the segment was assigned to the field sample
 288 covering the greater part of the segment. If less than 10% of the image segment was covered by the sample
 289 polygon, the segment was not assigned at all.

290

291 3.4.4 Predictive mapping

292 Besides the validation of the models, quality control of the prediction for not sampled trees was applied. The
 293 predicted tree species of both study areas were visually inspected within the corresponding tree covers. For both
 294 study areas species maps were produced showing the most probable tree species if the modeled probability
 295 exceeded 90%.

296

297 4. Results

298

299 4.1 Explanatory power of the variables

300 Tables 5 and 6 illustrate the explanatory power of the variables as suggested by the significant terms output by
 301 the *mlogit*.

302

303 **Table 5.** Counts of significant ($P < 0.05$) contributions of variable groups for study area 1. The group of geometric
 304 variables includes curvature and slope.

Variable groups	<i>Acer sp.</i>	<i>Alnus sp.</i>	<i>Betula sp.</i>	<i>Fagus</i> <i>sylvatica.</i>	<i>Fraxinus</i> <i>excelsior</i>	<i>Abies alba</i> <i>abies</i>	<i>Picea</i>	Total
RC30-CIR	-	2	1	4	6	2	1	16
RC30-CIR-Ratio	-	2	1	2	5	2	3	15

RC30-CIR-IHS	-	5	-	-	4	-	3	12
ADS40-RGB	-	4	1	1	4	7	2	19
ADS40-RGB-Ratio	-	3	1	-	1	2	2	9
ADS40-RGB-IHS	-	5	1	1	1	1	2	11
Geometric	-	7	1	4	2	4	4	22

Table 6. Counts of significant ($P < 0.05$) contributions of variable groups for study area 2. All variables are derived from the ADS40-SH52 data. The group of geometric variables includes curvature, aspect and slope.

Variable groups	<i>Betula sp.</i>	<i>Larix decidua</i>	<i>Picea abies</i>	<i>Pinus sylvestris</i>	Total
IHS-RGB	-	4	2	3	9
IHS-CIR	-	7	1	4	12
Geometric	-	2	3	2	7

Tables 5 and 6 reveal that all variable groups contributed significant terms. Geometric variables and the RGB bands of the ADS40-SH40 data (study area 1) and IHS of the CIR bands of the ADS40-SH52 data (study area 2) seem to be particularly informative. For *Acer sp.* (study area 1) and for *Betula sp.* (study area 2), no significant terms were found.

4.2. Step-wise variable selection

The counts of significant terms remaining in separate logistic models for each tree species after step-wise variable selection are shown in Tables 7 and 8.

Table 7. Counts of significant ($P < 0.05$) contributions of variable groups for study area 1

Variable groups	<i>Acer sp.</i>	<i>Alnus sp.</i>	<i>Betula sp.</i>	<i>Fagus sylvatica.</i>	<i>Fraxinus excelsior</i>	<i>Abies alba</i>	<i>Picea abies</i>	
RC30-CIR	5	-	-	8	10	-	10	33
RC30-CIR-Ratio	6	-	-	6	11	-	4	27
RC30-CIR-IHS	8	-	-	7	7	-	6	28

ADS40-RGB	5	-	-	7	8	-	6	26
ADS40-RGB-Ratio	6	-	-	5	6	-	7	24
ADS40-RGB-IHS	3	-	-	7	5	-	8	23
geometric	8	-	-	2	9	-	10	29

Table 8. Counts of significant ($P < 0.05$) contributions of variable groups for study area 2. All variables are derived from the ADS40-SH52 data.

Variable groups	<i>Betula sp.</i>	<i>Larix decidua</i>	<i>Picea abies</i>	<i>Pinus sylvestris</i>	Total
RGB	-	5	7	4	16
CIR	-	4	8	7	19
Ratio-RGB	-	9	7	5	21
Ratio-CIR	-	9	9	7	25
IHS-RGB	-	4	8	7	19
IHS-CIR	-	3	5	8	16
geometric	-	8	8	4	20

Tables 7 and 8 reveal that all variable groups contributed significant terms. CIR bands of the RC30 data (study area 1) and of the ADS40-SH52 data (study area 2) or their ratios seem to be particularly informative. For *Abies alba*, *Acer sp.*, and *Alnus sp.* (study area 1) and for *Betula sp.* (study area 2), no significant terms were found.

4.3. Cross-validation

Neuronal network models for all tree species were ten-fold cross-validated using the different explanatory variable groups. For study area 1 best CCR and K are obtained when using the means and standard deviations of all variables (table 9 left). Best accuracies for study area 2 are obtained when using the original RGB and CIR bands both ADS40-SH52 (table 9 right). The results clearly show that the single usage of geometric variables is not very contributive for the classification of tree species (study area 1: $K = 0.13$, study area 2: $K < 0$). For study area 1 up to 10% higher accuracies are obtained when using explanatory variables from both the ADS40-SH40 and RC30 imagery.

335

336 **Table 9.** Overview of ten-fold cross-validation of the neuronal network models for all tree species based on different
337 variable groups. The RGB variables are obtained from the ADS40-SH40 (study area 1) and the ADS40-SH52 data (study
338 area 2). The CIR variables are obtained form RC30 (study area 1) and ADS40-SH52 data (study area 2).

Variable groups	Study area 1		Study area 2	
	<i>CCR</i>	<i>K</i>	<i>CCR</i>	<i>K</i>
Geom. variables	0.351	0.133	0.532	-0.150
RGB	0.663	0.552	0.780	0.631
CIR	0.652	0.539	0.808	0.684
Ratio RGB	0.663	0.552	0.780	0.631
Ratio CIR	0.576	0.424	0.804	0.676
RGB & CIR	0.712	0.625	0.831	0.729
ratio RGB & CIR	0.682	0.579	0.821	0.707
IHS RGB	0.685	0.583	0.779	0.622
IHS CIR	0.560	0.403	0.800	0.672
IHS RGB & CIR	0.705	0.615	0.824	0.713
all variables	0.762	0.698	0.765	0.635

339

340

341 *4.4 Confusion matrices*

342 The confusion matrices of the models with best *CCR* and *K* are summarized in Tables 10 and 11.

343 **Table 10.** Confusion matrix for tree species classification (ten-fold cross-validated) in study area 1 using all geometric and
344 spectral explanatory variables (mean and standard deviations of ADS40-SH40 and RC30 imagery) with the producer's- and
345 user's accuracy of the classified tree segments of different tree species, *CCR*, and Cohen's kappa coefficient (*K*). The total
346 number of segments is 955, of which 76% were correctly classified

347

Field data		Classified as							producer's accuracy %	<i>K</i>
Study area 1	<i>Acer sp.</i>	<i>Alnus</i>	<i>Betula</i>	<i>Fagus</i>	<i>Fraxinus</i>	<i>Abies</i>	<i>Picea</i>			
ADS40-SH40 + RC30		<i>sp.</i>	<i>sp.</i>	<i>sylvatica</i>	<i>excelsior</i>	<i>alba</i>	<i>abies</i>			
<i>Acer sp.</i>	17	2	2	21	15	4	6	25.4		
<i>Alnus sp.</i>	3	27	-	7	3	-	1	65.9		

<i>Betula sp.</i>	1	2	14	4	-	1	5	51.9
<i>Fagus sylvatica.</i>	15	14	4	233	9	5	9	80.6
<i>Fraxinus excelsior</i>	10	5	2	14	120	-	2	78.4
<i>Abies alba</i>	2	0	2	7	-	107	12	82.3
<i>Picea abies</i>	2	4	7	11	2	12	210	84.7
User's accuracy %	34.0	0.5	45.2	78.5	80.5	83.0	85.7	
CCR							0.76	0.70

348

349 Table 10 shows that best agreements are obtained for *Picea abies* (84.7%), *Abies alba* (82.3%), *Fagus sylvatica*
350 (80.6%), and *Fraxinus excelsior* (78.4%). Only few *Abies alba* are misclassified as *Picea abies* and few
351 *Fraxinus excelsior* as *Fagus sylvatica*, respectively. The most frequent failures happen in classifying the non-
352 dominant tree species *Acer sp.*, *Alnus sp.*, and *Betula sp.*, which are often misclassified as the two dominant
353 deciduous tree species *Fagus sylvatica* and *Fraxinus excelsior*. The obtained accuracies remain lower for the
354 non-dominant tree species.

355 The confusion matrix for the four classified tree species in study area 2 is summarized in table 11. It shows a
356 high overall accuracy and a high kappa value.

357

358 **Table 11.** Confusion matrix for tree species classification (ten-fold cross-validated) in study area 2 using the 12
359 explanatory variables (mean and standard deviation of the RGB and CIR bands) from ADS40-SH52 imagery with the
360 producer's- and user's accuracy of the classified tree species, CCR, and Cohen's kappa coefficient (*K*). The total number of
361 segments is 801, of which 84% were correctly classified.

362

Field data	Classified as					
Study area 2	<i>Betula sp.</i>	<i>Picea abies</i>	<i>Pinus</i>	<i>Larix</i>	producer's	<i>K</i>
ADS40-SH52			<i>sylvestris</i>	<i>decidua.</i>	accuracy %	
<i>Betula sp</i>	58	7	3	7	77.6	
<i>Picea abies</i>	9	33	40	16	33.7	
<i>Pinus sylvestris</i>	4	10	169	12	86.7	

<i>Larix decidua</i>	3	9	11	409	94.7
User's accuracy %	78.7	55.9	75.8	92.1	
<i>CCR</i>					0.84
					0.74

363

364 The analysis revealed that best agreements are obtained for *Larix decidua* (94.7%), *Pinus sylvestris* (86.7%),
365 and *Betula sp.* (77.6%). The accuracy for *Picea abies* is lower (33.7%). It is often misclassified as *Pinus*
366 *sylvestris* and less frequently as *Larix decidua*.

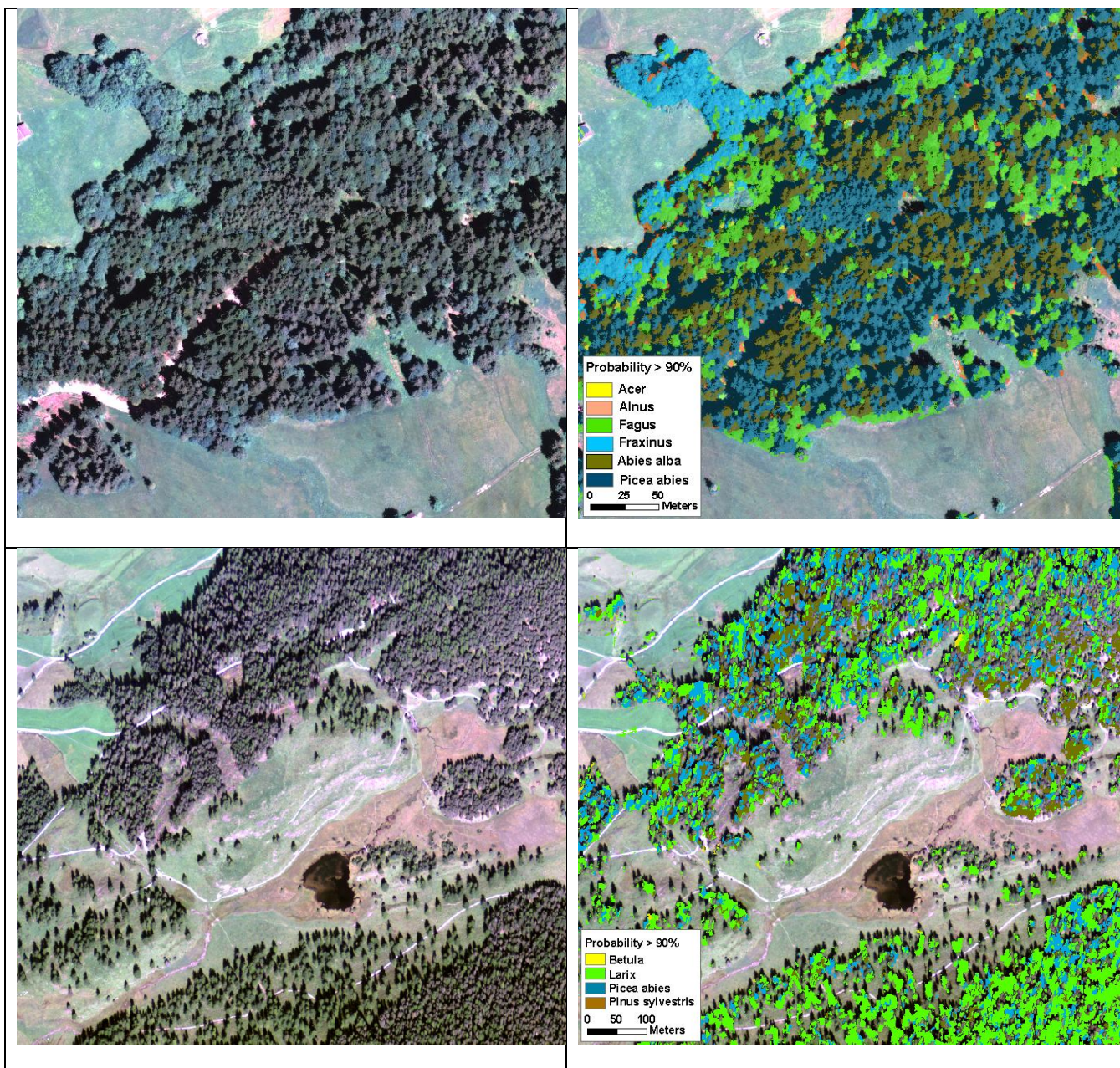
367

368 4.5 Predictive mapping

369 The tree species which have been modeled with > 90 % probability in study area 1 and 2 are depicted in Fig. 4.
370 For a better visualization not all tree species are shown in study area 1. At first glance, a visual image analysis
371 suggests that the agreements in most parts of the site are good. However, a more detailed image inspection
372 confirms the results of table 10 and indicates that *Acer sp.* and *Alnus sp.* are often misclassified as *Fagus*
373 *sylvatica* or *Fraxinus excelsior*. Fig. 4 clearly shows that *Fraxinus excelsior* (light blue) is overestimated along
374 forest borders in the upper left part of study area 1. Thus, the few *Acer sp.* and *Alnus sp.* are difficult to
375 recognize.

376 In study area 2, a slight underestimation of *Picea abies* in favour of *Larix decidua* in the lower right part is
377 visible. Apart from these misclassifications *Larix decidua*, *Pinus sylvestris* and *Betula sp.* show few
378 mispredictions.

379



380

381

382

383

384

385

386

Figure 4. Top left: Part of ADS40-SH40 RGB orthoimage (histogram equalized) of study area 1. Top right: Classification with tree species > 90% probability based on ADS40-SH40 and RC30 explanatory variables. Bottom left: Part of ADS40-SH52 RGB orthoimage (histogram equalized) of study area 2. Bottom right: Classification with tree species > 90% probability. For both classification maps: tree segments which have < 90% probability of a tree species are not colored.

5. Discussion and conclusions

387

388 The potential and the limits of classifying the dominant tree species has been tested in two study areas with
389 different terrain and forest conditions. The most significant achievement is the demonstration that multispectral
390 ADS40-SH52 imagery with multinomial regression models proved to have a high potential to produce
391 meaningful tree species classifications with a minimum effort involved in image acquisition, data pre-
392 processing, derivation of explanatory variables and field work. Promising classification results for 4-7 different
393 tree species were confirmed with ground information and what can be seen visually on the imagery. However,
394 this study also has some limitations which are briefly discussed below.

395

396 *5.1 Ground truth*

397 The tree samples were delineated in the field on aerial images, which means that well visible trees may have
398 been preferred, or only the lighted parts of trees have been delineated. Additionally, trees may be shaded or
399 partly hidden by others so that one image segment could contain more than one species. These uncertainties
400 render the statistical evaluations relative. As long as models of the same data sets are compared, the results can
401 be interpreted as declared in section 3.4.1. However, when comparing correct classification rates or kappa
402 values to other studies, we emphasize that this is a qualitative approach. For the same reasons the model results
403 were checked for plausibility by visual examination of the aerial photographs.

404

405 *5.2 Model choice and variable selection*

406 Since parametric models enable easy and experienced variable selection procedures and model diagnostics as
407 well, the usage of GLMs was considered.

408 According to Guisan et al. (2002) step-wise variable selection with the AIC criterion is often used as an analytic
409 tool to find redundant explanatory variables which are then excluded from the model. However, the AIC
410 criterion is adapted to linear models and should be handled with reservation when modeling in a transformed
411 data space (e.g. GLMs).

412 In the present study, variable selection was misleading, suggesting that also geometric variables are powerful
413 explanatory variables (see tables 7 and 8). The results of ten-fold cross-validations for all modeled tree species
414 were different and revealed that for study area 1 geometric variables only in combination with the spectral
415 variables and for study area 2 the original variables of RGB and CIR bands performed best. A real contribution
416 of geometric variables to classify tree species was only obtained in study area 1. The reason for this might be the
417 higher spatial resolution (0.25 m in contrary to 0.5 m in study area 2) of the canopy height model in area 1.

418

419 *5.3 Comparison with other studies*

420 Overall, the accuracies obtained in this study are in line with or higher than those in similar studies. However, a
421 direct comparison is difficult due to the following aspects: 1) Higher accuracies are obtained with fewer species
422 classes; 2) higher accuracies are obtained when inappropriate or no cross-validation is applied, 3) tree species
423 classification is based on other sensors; and 4) the forest structure and tree species composition (affected by the
424 alpine topography) of the two study areas seem to be more complex than they are in most similar studies.

425 Overall accuracies between 75% and 89% are obtained in studies involving the multispectral classification of
426 different coniferous species and one deciduous species. Our overall accuracy of 84% for four tree species in
427 study area 2 is therefore placed in the upper range. Overall accuracies around 75% are obtained in most studies
428 using CIR aerial images to classify Norway spruce, Scots pine, birch and aspen. E.g. Erikson (2004) obtained an
429 overall accuracy of 77% and Brandtberg (2002) between 67% and 79%. Key et al. (2001) obtained an overall
430 accuracy of 75% for the classification of four deciduous tree species using multi-temporal CIR aerial images.
431 Olofsson et al. (2006) used multispectral imagery taken with a Zeiss/Intergraph DMC camera and obtained 88%
432 overall accuracy to discriminate between Scots pine, Norway spruce and deciduous trees. Obviously,
433 classification accuracies are lower the more tree species there are and if non-dominant tree species are included.
434 In our study, the best overall correct classification (76%) was for seven tree species in study area 1, obtained
435 using both ADS40-SH40 and RC30 data. Chubey et al. (2009) found a classification of 4-6 coniferous and 4-6
436 deciduous species in Canadian forests (based on training by interpreters) to be 60-70% accurate.

437 In other studies, using tree-specific information from DSM obtained from very high resolution laser data (> 6
438 points / m^2) has been found to improve the classification of tree species substantially. For example, Ørka et al.
439 (2009) obtained an overall classification accuracy of 88% for birch and spruce, and Heinzl et al. (2008) of 84%
440 for discriminating between coniferous trees, beech and oak/hornbeam, when LiDAR was combined with CIR
441 true orthoimages. Holmgren et al. (2008) obtained an overall accuracy of 96% when classifying groups of
442 Norway spruce, Scots pine, and deciduous trees, using autumn multispectral images from Z/I DMC camera in
443 combination with very high-resolution LiDAR data (50 points / m^2). For the Swiss NFI and the Swiss Mire
444 Protection Program this is less relevant since such dense LiDAR data is unlikely to be available for the whole
445 country in the near future.

446

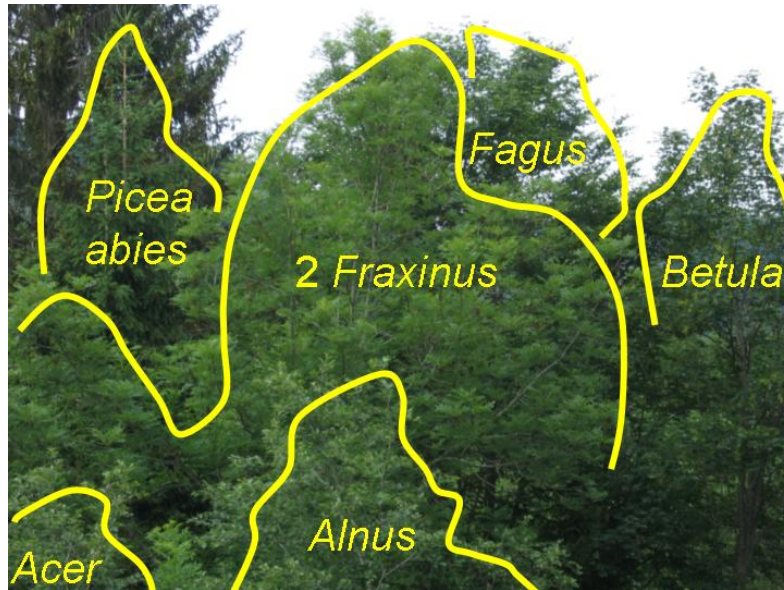
447 5.4 Non-dominant tree species

448 Although we found that in general our approach is very suitable for classifying tree species in different types of
449 forest, a more detailed analysis of the misclassifications is needed. Table 10 clearly reveals that most frequent
450 failures happen in classifying the non-dominant tree species. A reason for this was the relatively small sample
451 size of these non-dominant tree species - compared to the other species in a study area – which led to
452 underestimation of these species. Another reason is that non-dominant tree species are often short and therefore
453 partly obscured by nearby large and dominant trees, or by the merging of close crowns.

454 Field visits in study area 1 and visual stereo-image interpretation revealed that these non-dominant tree species
455 *Acer sp.*, *Alnus sp.* and *Betula sp.* are often not grouped, have smaller crowns and are therefore partly covered
456 by each other or by other more dominant species. Fig. 5 illustrates this situation. Visual analysis of the spectral
457 ranges of each species moreover revealed very similar spectral properties between *Alnus sp.* and *Acer sp.* Even
458 within species, spectral variability can be large because of illumination and view-angle conditions, openness of
459 trees, natural variability, shadowing effects and differences in crown health. Spectral separability between
460 species and the variability of trees within species have also been analysed and described in Leckie et al. (2005).

461 To overcome these problems, our approach is currently being tested in another study area using multi-temporal
462 ADS40-SH52 images to separate non-dominant tree species with spectral similarities.

463



465

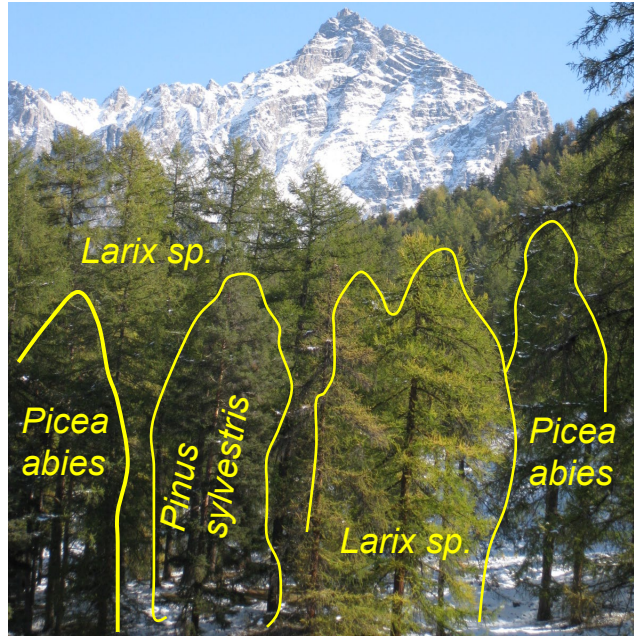
466 **Figure 5.** Illustration to show the problems involved in identifying small and non-dominant deciduous trees in study area 1.

467 The group of *Fraxinus excelsior* partly covers small trees like *Acer sp.* and *Alnus sp.*, at the background *Picea abies* and
468 *Fagus sylvatica* are dominant, whereas *Betula sp.* is characterized by having a small crown diameter.

469

470 While misclassifications in study area 1 are mostly restricted to the non-dominant tree species, most errors in
471 study area 2 involved *Picea abies* mostly being misclassified as *Pinus sylvestris* and less as *Larix decidua*. This
472 was not surprising since the spectral signatures of *Picea abies* and *Pinus sylvestris* tend to overlap considerably,
473 especially in the partly shaded areas (see Fig. 6).

474 Visual image inspection reveals that *Picea abies* is often partly covered by dominant larches at forest borders
475 but correctly classified in open land. Additionally, interviews with local foresters revealed that at the time of
476 recording the images of 2008, the vitality of the larches was affected by larch bud moth attack which could also
477 explain the spectral similarity between *Larix decidua* and *Picea abies*.



478

479 **Figure 6.** Illustration to show the problems involved in identifying *Picea abies* in study area 2. Both *Picea abies* and *Pinus*
 480 *sylvestris* are partly covered by large and dominant *Larix decidua* trees. Although having a small crown diameter, *Pinus*
 481 *sylvestris* is classified with higher accuracy than *Picea abies*.

482

483 5.5 Operational use for the Swiss NFI

484 The promising results and experiences made in this study are of great practical interest since many tasks
 485 necessary for the Swiss National Forest Inventory (e.g. support for stereo-interpretation of sample plots) and the
 486 Swiss Mire Monitoring Program (e.g. assessment of growth influence of certain tree species on mires) are based
 487 or will be based on these imagery. Actual and accurate maps of tree species and composition are needed by
 488 environmental agencies and land surveying offices to assess possible changes in species distribution or condition
 489 of other habitats. Currently, the tree species classification approach is being tested in other Swiss regions with
 490 the ADS40-SH52 and ADS80 sensor which has been in use since 2009. Continuity of this approach is
 491 guaranteed since the necessary input data (ADS40 / ADS80 imagery) is collected every three years nationwide
 492 by the Federal Geo-Information center (SWISSTOPO) and the classification of tree species will be based on the
 493 same sensors. Furthermore, the required segmentation of these images will be performed in-house in the

494 framework of other monitoring programs. Lots of cost-effective and additional field work won't be needed since
495 in-house existing or currently collected field samples of tree species elsewhere in Switzerland can be used.
496 According to experts of the Swiss NFI, the classification accuracies obtained in this study are sufficient –
497 especially regarding that no area-wide information on tree species distribution is available yet. Although the
498 forest area of the two study areas ($\approx 4 \text{ km}^2$) is very small compared to the entire national forest area of approx.
499 $12'700 \text{ km}^2$, this semi-automatic classification approach is a valuable contribution since the methods developed
500 in this study can be easily adapted to other forest areas. However, before this approach is used operationally, it
501 should be tested for large areas ($> 1000 \text{ km}^2$).

502

503 **6. Outlook**

504

505 The most obvious opportunities for follow up are listed below:

- 506 - NFI sample plots as training data will be used to reduce field work.
- 507 - Further development is needed for testing larger areas, which may consist of several image strips recorded
508 with the trees having a different phenological status. For this, radiometric correction within and between
509 images strips should be taken into account as well as it is already performed e.g. in Chubey et al (2009).
- 510 - Further research is needed to improve distinguishing non-dominant tree species. This should also include
511 multi-temporal imagery for a better distinction of deciduous trees with spectral similarities. BRDF-related
512 problems or influences of the BRDF in terms of classification accuracy should also be investigated.

513

514 **Acknowledgements**

515

516 The study was carried out within the framework of the Swiss National Forest Inventory (NFI) and the Swiss
517 Mire Protection Program at the Swiss Federal Research Institute WSL. It was funded by the Swiss Federal
518 Office for the Environment (FOEN) and WSL. We are grateful to Patrick Thee for his valuable help in the field
519 surveys, and to Adrian Lanz from the Swiss NFI for fruitful discussions while preparing the manuscript. Finally,

520 we thank Silvia Dingwall for the English revision of the manuscript and two anonymous reviewers for helpful
521 comments on an earlier version of this manuscript.

522

523 **References**

524

525 Akaike, H. (1973). Information theory as an extension of the maximum likelihood principle. In: Petrov, B.N.,
526 Csaki, F. (eds.), *Second International Symposium on Information Theory*. Akademiai Kiado, Budapest,
527 Hungary, pp. 267-281.

528

529 Artuso, R., Bovet, S., & Streilein, A. (2003). Practical Methods for the Verification of countrywide Terrain and
530 Surface Models, In: *International Archives of Photogrammetry and Remote Sensing*, vol. XXXIV-3/W13

531

532 Baatz, M., & Schäpe, A. (2000). Multiresolution Segmentation – an optimization approach for high quality
533 multi-scale image segmentation. In J. Strobl, T. Blaschke and G. Griesebner (eds.), *Angewandte Geographische*
534 *Informationsverarbeitung Vol. XII* (pp. 12-23). Heidelberg, Germany: Wichmann

535

536 Baltsavias, E., Gruen, A., Eisenbeiss, H., Zhang, L., & Waser, L.T. (2008). High Quality Image Matching and
537 Automated Generation of 3D Tree Models. *International Journal of Remote Sensing*, 29(5), 1243 - 1259

538

539 Bolduc, P., Lowell, K., & Edwards, G. (1999). Automated estimation of localized forest volume from large-
540 scale aerial photographs and ancillary cartographic information in a Boreal forest. *International Journal of*
541 *Remote Sensing*, 20, 3611- 3624

542

543 Brandtberg, T. (2002). Individual tree-based species classification in high spatial resolution aerial images of
544 forests using fuzzy sets. *Fuzzy Sets and Systems*, 132, pp 371-387

545

546 Brandtberg, T. (2007). Classifying individual tree species under leaf-off and leaf-on conditions using airborne
547 LiDAR. *ISPRS Journal of Photogrammetry and Remote Sensing*, 61, 325-340

548

549 Brassel, P., & Lischke, H. (2001). *Swiss National Forest Inventory: methods and models of the second*
550 *assessment*, Swiss Federal Research Institute WSL, Birmensdorf. 336 p.

551

552 Burrough, P.A. (1986). *Principles of Geographical Information Systems for Land Resources Assessment*. New
553 York: Oxford University Press, 50 p.

554

555 Chubey, M., Stehle, K., Albricht, R., Gougeon, F., Leckie, D., Gray, S., Woods, M., & Courville, P. (2009).
556 Semi-Automated Species Classification in Ontario Great Lakes - St. Lawrence Forest Conditions. Final Report:
557 Great Lakes - St. Lawrence ITC Project (2005/2008). Ontario Ministry of Natural Resources. January 2009. 71
558 p.

559

560 DeKok, R., & Wezyk, P. (2006). Process development and sequential image classification for automatic
561 mapping using cas studies in forestry, *EARSeL-Proceedings of the Workshop on 3D Remote Sensing in Forestry*
562 *(pp. 380-384)*, 14th-15th Feb., 2006, Vienna, Austria.

563

564 Ecker, K., Küchler, M., Feldmeyer-Christe, E., Graf, U., & Waser, L.T., (2008).
565 Predictive mapping of floristic site conditions across mire habitats: Evaluating data requirements.
566 *Community Ecology*, 9 (2), 133-146

567

568 Erikson, M. (2004). Species classification of individually segmented tree crowns in high-resolution aerial
569 images using radiometric and morphologic image measures. *Remote Sensing of Environment*, 91, 469-477

570

571 Gillis, M., & Leckie, D. (1996). Forest inventory update in Canada. *The Forestry Chronicle*, 72, 138-156

572

573 Gonzales, R.C., & Woods, R.E. (2002). *Digital image processing*. Second edition. New Jersey: Upper Saddle
574 River

575

576 Guisan, A., Edwards, T.E., & Hastie, T. (2002). Generalized linear and generalized additive models in studies of
577 species distributions: setting the scene. *Ecological Modeling*, 157, 89-100.

578

579 Guisan, A., Weiss, S.B., & Weiss, A.D. (2004). GLM versus CCA spatial modeling of plant species distribution.
580 *Plant Ecology* 143(1), 107-122.

581

582 Guisan, A., & Zimmermann, N.E. (2000), Predictive habitat distribution models in ecology. *Ecological*
583 *Modeling*, 135(2-3), 147-186.

584

585 Guisan, A., & Thuiller, W. (2005). Predicting species distribution: offering more than simple habitat models.
586 *Ecology Letters*. 8, 993-1009

587

588 Heinzl, J.N., Weinacker, H., & Koch, B. (2008). Full automatic detection of tree species based on delineated
589 single tree crowns – a data fusion approach for airborne laser scanning data and aerial photographs, *Proceedings*
590 *of the SilviLaser 8th international conference on LiDAR applications in forest assessment and inventory*, (pp.
591 76-85), September 18-19, 2008, Edinburgh, UK.

592

593 Hirschmugl, M., Ofner, M., Raggam, J., & Schardt, M. (2007). Single tree detection in very high-resolution
594 remote sensing data. *Remote Sensing of Environment*, 110, 533-544

595

596 Holmgren, J., & Persson, Å. (2004). Identifying species of individual trees using airborne laser scanner. *Remote*
597 *Sensing of Environment*, 90, 415-423

598

599 Holmgren, J., Persson, Å., & Söderman, U. (2008). Species identification of individual trees by combining high
600 resolution LiDAR data with multispectral images. *International Journal of Remote Sensing*, 29, 1537-1552

601

602 Hosmer, D.W., & Lemeshow, S. (2000). *Applied logistic regression*, 2nd edition, New York: Wiley, 373 p.

603

604 Jensen, J.R. (2005). Introductory digital image processing: A remote sensing perspective - Prentice Hall, Upper
605 Saddle River, NY.

606

607 Kellenberger, T. W., Buehler, Y. A., Kneubuehler, M., & Ackermann, N. (2007). Auswertung von ADS40
608 Scanner-Daten im Testgebiet Vordemwald: - ADS40 System Data Processing For Remote Sensing Applications
609 - Objektorientierte Klassifikation Des Landwirtschaftsgebietes. RSL - Remote Sensing Laboratories-
610 Geographisches Institut, 52

611

612 Kellenberger, T. W., & Nagy, P. (2008). Potential of the ADS40 Aerial Scanner for Archaeological Prospection
613 in Rheinau, Switzerland. *Proceedings of XXI Congress International Society for Photogrammetry and Remote*
614 *Sensing 3-11 July 2008*, Beijing China

615

616 Key, T., McGra, J.B., & Fajvan, M.A. (2001). A comparison of multispectral and multitemporal information in
617 high spatial resolution imagery for classification of individual tree species in a temperate hardwood forest.
618 *Remote Sensing of Environment*, 75, 100-112

619

620 Küchler, M., Ecker, K., Feldmeyer-Christe, E., Graf, U., Küchler, H., & Waser, L.T. (2004). Combining
621 remotely sensed spectral data and digital surface models for fine-scale modelling of mire ecosystems.
622 *Community Ecology*, 5(1), 55-68.

623

624 Lamonaca, A., Corona, P., & A. Barbati, A. (2008). Exploring forest structural complexity by multi-scale
625 segmentation of VHR imagery. *Remote Sensing of Environment*, 112(6), 2839-2849

626

627 Leckie, D.G., Tinis, S., Nelson, T., Burnett, Ch., Gougeon, F.A., Cloney, E., & Paradine, D. (2005). Issues in
628 species classification of trees in old growth conifer stands. *Canadian Journal of Remote Sensing*, 31(2), 175-190

629

630 McCullagh, P., & Nelder, J.A. (1983). *Generalized linear models*. London: Chapman and Hall, 511 p

631

632 McLachlan, G. (1992). *Discriminant Analysis and Statistical Pattern Recognition*. Wiley, New York.

633

634 Moore, I. D., Grayson, R. B., & Landson, A. R., (1991). Digital Terrain Modelling: a Review of Hydrological,
635 Geomorphological, and Biological Applications. *Hydrological Processes*. Vol. 5., pp 3-30

636 Olofsson, K., Wallermann, J., Holmgren, J., & Olsson, H. (2006). Tree species discrimination using Z/I DMC
637 imagery and template matching of single trees. *Scandinavian Journal of Forest Research*, 21, 106-110

638

639 Ørka, H.O., Næsset, E., & Bollandsås, O.M. (2009). Classifying species of individual trees by intensity and
640 structural features derived from airborne laser scanner data. *Remote Sensing of Environment*, 113(6), 1163-1174

641

642 Petrie, G. & Walker, A.S. (2007). Airborne digital imaging technology: A new overview, *Photogrammetric*
643 *Record*, 22(119), 203-225

644

645 Reulke, R., Becker, S., Haala, N., & Tempelmann, U. (2006). Determination and improvement of spatial
 646 resolution of the CCD-line-scanner system ADS40. *ISPRS Journal of Photogrammetry & Remote Sensing*, 60,
 647 81–90
 648
 649 Scott, J.M., Heglund, P.J., Samson, F., Haufler, J., Morrison, M., & Wall, B. (2002). *Predicted species*
 650 *occurrences: issues of accuracy and scale*. Covelo, California: Island Press, 868
 651
 652 St-Onge, B., Jumelet, J., Cobello, M., & Vega, C. (2004). Measuring individual tree height using a combination
 653 of stereophotogrammetry and lidar. *Canadian Journal of Forest Research*, 34(10), 2122-2130
 654
 655 Straub, B. (2003). Automated Extraction of Trees from Aerial Images and Surface Models, In: *The International*
 656 *Archives of Photogrammetry and Remote Sensing*, XXXIV-3/W8, pp.157-164
 657
 658 Spurr, S.H. (1960). *Photogrammetry and Photo-Interpretation*, (pp. 382–392). Second edition. New York:
 659 Ronald Press
 660
 661 Wang, Y., Soh, Y.S., & Schultz, H. (2006). Individual tree crown segmentation in aerial forestry images by
 662 mean shift clustering and graph-based cluster merging. *International Journal of Computer Science and Network*
 663 *Security*, 6 (11), 40-45
 664
 665 Waser, L.T., Kuchler, M., Ecker, K., Schwarz, M., Ivits, E., Stofer, S., & Scheidegger, C. (2007). Prediction of
 666 Lichen Diversity in an Unesco Biosphere Reserve - Correlation of high Resolution Remote Sensing Data with
 667 Field Samples. *Environmental Modeling & Assessment*, 12(4), 315-328
 668
 669 Waser, L.T., Baltsavias, E., Ecker, K., Eisenbeiss, H., Ginzler, C., Kuchler, M., Thee, P., & Zhang, L. (2008a).
 670 High-resolution digital surface models (DSM) for modelling fractional shrub/tree cover in a mire environment.
International Journal of Remote Sensing, 29(5), 1261 – 1276

671

672 Waser, L.T., Ginzler, C., Kuechler, M., & Baltsavias, E. (2008b). Potential and limits of extraction of forest
673 attributes by fusion of medium point density LiDAR data with ADS40 and RC30 images. *Proceedings of the*
674 *SilviLaser 8th international conference on LiDAR applications in forest assessment and inventory*, (pp. 625-
675 634), *September 18-19, 2008, Edinburgh, UK*

676

677 Waser, L.T., Baltsavias, E., Ecker, K., Eisenbeiss, H., Feldmeyer-Christe, E., Ginzler, C., Kuechler, M., Thee, P.
678 & Zhang, L. (2008c). Assessing changes of forest area and shrub encroachment in a mire ecosystem using
679 digital surface models and CIR-aerial images. *Remote Sensing of Environment* 112(5): 1956-1968

680

681 Waser, L.T., Klonus, S., Ehlers, M., Kuechler, M. & Jung, A. (2010). Potential of digital sensors for land cover
682 and tree species classifications – a case study of the DGPF-project. *Photogrammetrie, Fernerkundung und*
683 *Geoinformation* 2, 141-156.

684

685 Wulder, M., (1998). Optical remote-sensing techniques for the assessment of forest inventory and biophysical
686 parameters. *Progress in Physical Geography* 22, 449-476

687

688 Zhang, L., & Gruen, A. (2004). Automatic DSM generation from linear array imagery data. *The International*
689 *Archives of Photogrammetry, Remote Sensing and Spatial Information Sciences*, XXXV, Part B3, (pp 128-133)

690